THE JOURNAL OF PHYSICAL CHEMISTRY B
A JOURNAL OF THE AMERICAN CHEMICAL SOCIETY

pubs.acs.org/JPCB

Article

Rheology of Ring Copolymers in Dilute Solutions

Sumit Kumar and Parbati Biswas*

Cite This: J. Phys. Chem. B 2025, 129, 496−505

Read Online

ACCESS | Metrics & More | Article Recommendations

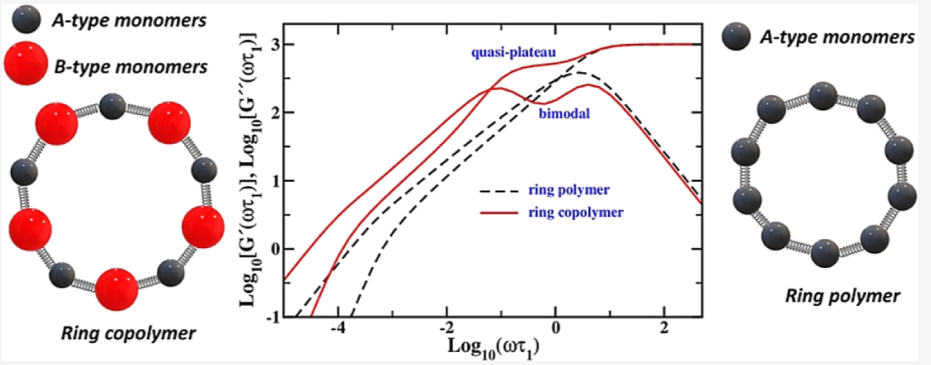

ABSTRACT: We investigate the rheology of ring copolymers theoretically within the framework of the optimized Rouse−Zimm theory in dilute solutions. The ring copolymer is composed of two type of monomers (A and B) of different sizes (A < B), which is represented by unequal-sized beads connected via harmonic springs with different spring constants. The hydrodynamic interactions (HI) between the monomers is modeled using the preaveraged HI tensor. These interactions accelerate the collective relaxation modes and impede the local relaxation modes. In the presence of HI, the storage modulus shows a quasi-plateau regime, demonstrating a viscoelastic solid-like response of the polymer, while the loss modulus exhibits a bimodal pattern due to the difference in the mobilities of the monomers. The inverse of the crossover frequency represents the overall characteristic relaxation time, which is higher for the ring copolymers than for the Rouse rings, suggesting a slower relaxation of the ring copolymers due to the presence of relatively large sized monomers. The quasi-plateau in the storage modulus and the bimodality in the loss modulus are enhanced with an increase in the size and number fraction of B-type monomers. An increase in the size of the B-type monomers increases both storage and loss moduli, resulting in an overall decrease in the dynamics of the ring copolymers.

1. INTRODUCTION

Ring polymers represent a distinct class of macromolecules characterized by their compact closed-loop architecture, devoid of free terminal ends, unlike linear polymers. This circular topology has a profound effect on the structure and dynamics of ring polymers both in melts and in solutions, making them distinctly different from their respective linear analogues. However, the presence of free chain ends plays a key role in understanding the dynamics of linear polymers. These free chain ends enable stress relaxation in melts and in concentrated solutions of linear polymers by reptation, unlike that of the ring polymers. Therefore, the rings are expected to exhibit a completely different dynamics.[1] The rheology of ring polymers is challenging not only from the point of view of developing new physics to elucidate the dynamics but also as a promising precursor to novel materials. Ring polymers are commonly prevalent in nature as bacterial DNA in mitochondria and plasmids and as circular prokaryotic genomes. Recent experimental methods have enabled the synthesis and characterization of ring polymers with precisely controlled size and topology,[2−5] thus permitting a detailed investigation of their conformation and dynamics, while various theoretical, simulation, and experimental studies have probed the conformation and dynamics of ring polymers in both solutions and melts,[6−11] and the properties of ring copolymers remain largely unexplored.

Ring copolymers are a unique class of polymers that comprise two or more different types of monomers connected in a ring. Such composite polymers incorporate multifunctional units within a single polymer and are expected to possess novel physical and chemical properties. The material properties of such hybrid polymers may be appropriately tuned by modulating the ratio or number fraction of the constituent monomers, which may be consequently tailored for specific

Received: August 28, 2024
Revised: November 22, 2024
Accepted: December 12, 2024
Published: December 19, 2024

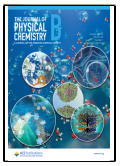

applications. However, these systems have not been investigated either experimentally or theoretically till date. The characterization and processability of the ring copolymers in dilute solutions rely on their small amplitude oscillatory shear material functions, such as the frequency(ω)-dependent storage modulus $G'(\omega)$, loss modulus $G''(\omega)$, and the time(t)-dependent stress relaxation spectrum $G(t)$.

This study reports the viscoelastic properties of the ring copolymers in dilute solutions within the tenets of the optimized Rouse−Zimm formalism. The ring copolymer is represented by a multiresolution bead−spring model where different-sized monomers are denoted as beads connected via harmonic springs with different spring constants. The solvent-mediated hydrodynamic interactions (HI) between the pair of monomers are incorporated through the preaveraged HI tensors. The viscoelastic properties of ring copolymers are measured in terms of the relaxation moduli, i.e., the storage modulus, $G'(\omega)$ and the loss modulus, $G''(\omega)$. The relaxation moduli are investigated as a function of the different sizes and number fractions of the two different monomers with and without HI. The characteristic relaxation time of a ring copolymer of a particular size with a specific number fraction is calculated from the frequency of crossover of the storage and loss moduli.

The review may be organized into the following sections: Section 2 of this paper outlines the theoretical formalism for the multiresolution bead−spring model of ring copolymers comprising unequal sized beads that are connected to each other through different harmonic springs. Section 3 describes the intramolecular relaxation dynamics of these copolymeric rings as a function of the size and number fraction of two different monomers with and without HI. Section 4 concludes by summarizing the major findings of this work.

2. THEORY

The ring copolymer is represented by a multiresolution bead−spring model, where the size of two different monomers, A and B, is denoted by beads of unequal sizes. The size of the B-type monomers is chosen to be greater than that of the A-type monomers. Both A- and B-type monomers are connected to each other by simple harmonic springs with different spring constants. A key parameter for determining the relative composition of B-type monomers in our system is the number fraction, which is the ratio of the number of B-type monomers N_B to the total number of A- and B-type monomers N_{total}. This number fraction ρ of the B-type monomers is expressed as $\rho = N_B/N_{total}$. For systems with $\rho = 0.5$, A- and B-type monomers are alternately connected and represent alternating ring copolymers ($ABAB$...). The systems with $\rho \neq 0.5$ represent the block ring copolymers ($A_xB_yA_xB_y$... with $(x, y) = (3,2)$ for $\rho = 0.4$, $(2,3)$ for $\rho = 0.6$, etc.), which are illustrated in Figure 1. Here, A- and B-type monomers are modeled as small and large sized beads. The friction coefficient of the monomers is proportional to their respective sizes as $\zeta_B = n\zeta_A$, where ζ_A and ζ_B are the friction coefficients of the A- and B-type monomers, respectively, and $n > 1$. For alternating ring copolymers, all bonds are considered to be of equal mean square length, with a spring constant given by $K = 3k_BT/l^2$, where k_B and T are the Boltzmann constant and temperature, respectively, and l^2 is the mean square length of the unstretched spring. The structure of the ring copolymer is represented by the $N \times N$ connectivity matrix, $[\boldsymbol{A}]$, which accounts for the connectivity of the monomers with different entropic springs. For $i \neq j$, element $\boldsymbol{A}_{ij}$ equals the number of entropic springs between i-th and j-th beads, if the i-th and j-th beads are connected and $\boldsymbol{A}_{ij} = 0$ otherwise. For $i = j$, the diagonal elements of connectivity matrix, $\boldsymbol{A}_{ii}$, are equal to the number of entropic springs connected to the i-th bead.[12−14]

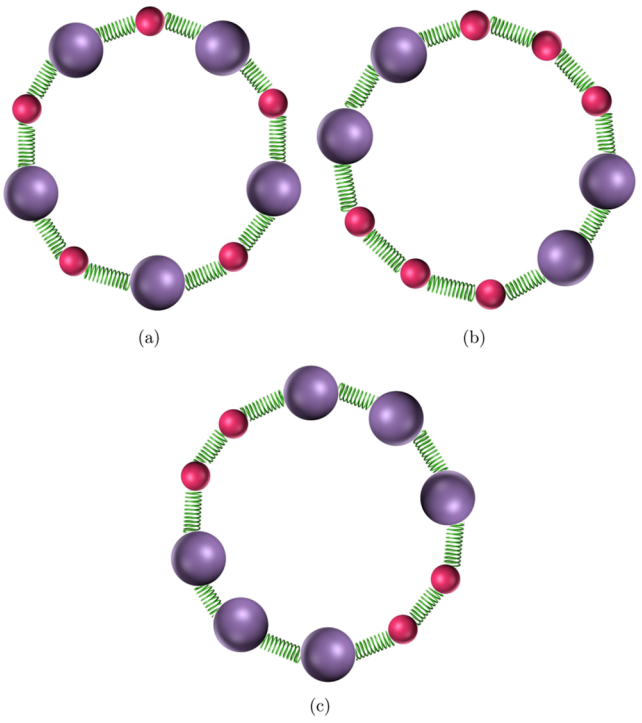

Figure 1. Ring copolymers with different number fractions (a) ρ = 0.5, (b) ρ = 0.4, and (c) ρ = 0.6.

The time evolution of the position coordinate of the i-th monomer of the ring copolymer, $\boldsymbol{R}_i(t)$, follows the overdamped Langevin equation, which may be expressed in the matrix form as[15,16]

$$\zeta_A \frac{\partial \boldsymbol{R}_i(t)}{\partial t} = -K \sum_{j=1}^{N} [\boldsymbol{H}.\ \boldsymbol{A}]_{ij} \boldsymbol{R}_j + \sum_{j=1}^{N} \boldsymbol{H}_{ij} \boldsymbol{f}_j(t) \quad (1)$$

Each monomer has a friction coefficient, $\zeta_j = 6\pi\eta_s a_j$, where a_j is the radius of the j-th monomer. These monomers are connected to each other via harmonic springs with the spring constant $K = 3k_BT/l^2$. The characteristic bond rate constant is given as $\sigma_0 = K/\zeta_A$. Here, $\boldsymbol{f}_j(t)$ represents the random force that accounts for the random thermal fluctuations with zero mean and delta correlation, i.e., $\langle \boldsymbol{f}_j(t) \rangle = 0$, $\langle \boldsymbol{f}_i(t) \boldsymbol{f}_j(t') \rangle = 2k_BT\zeta[\boldsymbol{H}^{-1}]_{ij}\delta_{ij}\delta(t - t')$, where $[\boldsymbol{H}^{-1}]$ is the inverse of the HI matrix, $[\boldsymbol{H}]$. This HI matrix, $[\boldsymbol{H}]$, takes into account the interaction between the monomers in dilute solutions. The elements of the matrix $[\boldsymbol{H}]$, $[\boldsymbol{H}_{ij}]$, describes the HI between the i-th and j-th monomers. The Oseen tensor and Rotne−Prager−Yamakawa (RPY) tensor are commonly used for approximating the HI. The Oseen tensor represents the HI between two point-like particles, which may be expressed as[15,16]

https://doi.org/10.1021/acs.jpcb.4c05788
J. Phys. Chem. B 2025, 129, 496−505

$$\boldsymbol{H}_{ij} = \begin{cases} \dfrac{\boldsymbol{I}}{6\pi\eta_s a}, & \text{for } i = j. \\ \dfrac{1}{8\pi\eta_s \boldsymbol{R}_{ij}}[\hat{\boldsymbol{R}}_{ij} \otimes \hat{\boldsymbol{R}}_{ij} + \boldsymbol{I}], & \text{for } i \neq j. \end{cases} \tag{2}$$

where $\boldsymbol{I}$ is the identity matrix and a is the radius of the bead. The distance between beads is given by $\boldsymbol{R}_{ij} = \boldsymbol{R}_i - \boldsymbol{R}_j$ and η_s representing the viscosity coefficient of the solvent. Additionally, $\hat{\boldsymbol{R}}_{ij}$ is the unit vector in the direction of $\boldsymbol{R}_{ij}$ and denoted by $\hat{\boldsymbol{R}}_{ij} = \frac{\boldsymbol{R}_i - \boldsymbol{R}_j}{|\boldsymbol{R}_{ij}|}$.

The RPY tensor accounts for the HI between the finite size beads. The elements of the HI matrix, $[\boldsymbol{H}_{ij}]$, are given by[17−19]

$$\boldsymbol{H}_{ij} = \begin{cases} \dfrac{1}{6\pi\eta_s a}, & \text{if } i = j. \\ \dfrac{1}{8\pi\eta_s \boldsymbol{R}_{ij}}\left[\left(1 + \dfrac{2a^2}{3\boldsymbol{R}_{ij}^{\,2}}\right)\boldsymbol{I} + \left(1 - \dfrac{2a^2}{\boldsymbol{R}_{ij}^{\,2}}\right)\right. & \text{if } 2a < \boldsymbol{R}_{ij}. \\ \left.\hat{\boldsymbol{R}}_{ij} \otimes \hat{\boldsymbol{R}}_{ij}\right], & \end{cases} \tag{3}$$

Equation 1 cannot be solved in the closed form by substituting the HI matrices defined by eq 2 or eq 3. For a tractable form of the HI tensor, a preaveraging approximation was introduced by Zimm,[20] where the elements of the HI matrix $\boldsymbol{H}_{ij}$ are replaced by its equilibrium average $\langle \boldsymbol{H}_{ij} \rangle$. The preaveraged hydrodynamic matrix, $\langle \boldsymbol{H}_{ij} \rangle$, is a constant where the fluctuations are neglected and may be solved using theoretical approaches similar to those developed for the free-draining limit of a polymer. The preaveraged form of both Oseen and RPY tensors have the same expression as given below[18,21,22]

$$[\boldsymbol{H}_{ij}] = \begin{cases} \dfrac{1}{6\pi\eta_s a_i}, & \text{for } i = j. \\ \dfrac{1}{6\pi\eta_s}\left\langle \dfrac{1}{\boldsymbol{R}_{ij}} \right\rangle_{\text{eq}}, & \text{for } i \neq j. \end{cases} \tag{4}$$

Therefore, the HI of the ring copolymer with unequal sized beads can be calculated through the preaveraged HI tensor as

$$[\boldsymbol{H}_{ij}] = (\delta_{ij}/\zeta_j + \zeta_r^{\,ij}\langle l/\boldsymbol{R}_{ij}\rangle(1 - \delta_{ij}))\boldsymbol{I} \tag{5}$$

where ζ_j is expressed in units of ζ_A. The HI between different segments depends upon their respective sizes and hence their friction coefficients (ζ), as given by $\zeta_r^{ij} = \zeta_r(\alpha_i + \alpha_j)/2$, where α_i and α_j depend on the hydrodynamically interacting beads and are considered 1 for the A-type monomer and greater than 1 for the B-type monomer in units of l.[13] The reduced monomer friction coefficient, $\zeta_r = \zeta/6\pi\eta_s l$, measures the strength of HI in units of l and η_s. The value of $\zeta_r = 0.25$ ensures the positive definiteness of the matrix $[\boldsymbol{H}]$.[23,24] The average intermonomer distances in eq 5 are assumed to be Gaussian distributed at equilibrium, and the averaged reciprocal intermonomer distances, $\langle \frac{1}{\boldsymbol{R}_{ij}} \rangle$, are approximated in terms of the mean square intermonomer distances, $\langle \boldsymbol{R}_{ij}^{\,2} \rangle$, as $\langle \boldsymbol{R}_{ij}^{-1} \rangle = \left(\frac{6}{\pi\langle \boldsymbol{R}_{ij}^{\,2} \rangle}\right)^{1/2}$. The mean square intermonomer distances are given as $\langle \boldsymbol{R}_{ij}^{\,2} \rangle = \sum_{k=1}^{N-1} \frac{(\boldsymbol{Q}_{ik} - \boldsymbol{Q}_{kj})^2}{\mu_k}$, where $\boldsymbol{Q}$ represents the eigenvectors of matrix $[\boldsymbol{H}.\boldsymbol{A}]$ and μ_k are the diagonal elements of the diagonal matrix, $\boldsymbol{Q}^T[\boldsymbol{H}.\boldsymbol{A}]\boldsymbol{Q}$, in the partial draining limit. In the absence of HI, the $N \times N$ matrix $[\boldsymbol{H}]$ is a diagonal matrix that accounts for the different sized beads with $[\boldsymbol{H}_{ij}] = \delta_{ij}/\zeta_j$. Therefore, it may be observed that the matrices $[\boldsymbol{H}]$ and $[\boldsymbol{A}]$ incorporate the effects of unequal sized beads connected by harmonic springs with different spring constants.[13,14]

Equation 1 is solved by decoupling into independent normal modes by numerically diagonalizing the matrix product $[\boldsymbol{H}.\boldsymbol{A}]$ using the QR algorithm.[25] This diagonalization yields N linearly independent eigenvectors $[\boldsymbol{Q}_k]$ such that $\boldsymbol{Q}^{-1}[\boldsymbol{H}.\boldsymbol{A}]\boldsymbol{Q} = \Lambda$, where Λ is a diagonal matrix with elements λ_k. The elements, λ_k, are the eigenvalues of the $[\boldsymbol{H}.\boldsymbol{A}]$ matrix and are directly proportional to the relaxation rates, $1/\tau_k$, of the normal relaxation modes. This same set of eigenvectors may also diagonalize the matrix $[\boldsymbol{A}]$ such that $\boldsymbol{Q}^T[\boldsymbol{A}]\boldsymbol{Q} = \Gamma$, where Γ is a diagonal matrix with elements λ_k^0.[26] The eigenvalues λ_k and λ_k^0 are real and nonnegative. The formalism of this theory is built from the generalized matrix $[\boldsymbol{H}.\boldsymbol{A}]$, which accounts for the unequal sized beads connected by different harmonic springs. When all friction coefficients and spring constants are equal, eq 1 reduces to that of a ring homopolymer.[27,28]

The rheology of the ring copolymers is typically characterized by the small amplitude oscillatory shear material functions that are evaluated from the complex shear relaxation modulus, $G^*(\omega) = G'(\omega) + \imath G''(\omega)$, which measures the response of any polymer to the applied harmonic strain as a function of the normalized frequency. The complex modulus is obtained from the Fourier transform of the relaxation modulus $G(t)$ as $G^*(\omega) = \int_0^\infty G(t)e^{-i\omega t}dt$. The complex modulus has two components, real and imaginary, which comprise the storage $(G'(\omega))$ and loss $(G''(\omega))$ modulus, respectively. $G'(\omega)$ and $G''(\omega)$ represent the frequency-dependent moduli that account for the relaxation dynamics of the polymer. These moduli may be expressed as dimensionless quantities as[29−32]

$$[G'(\omega)] = \frac{NG'(\omega)}{\nu k_B T} = \sum_{k=1}^{N-1} \frac{(\omega)^2}{(\omega)^2 + (2\sigma\lambda_k)^2} \tag{6}$$

$$[G''(\omega)] = \frac{NG''(\omega)}{\nu k_B T} = \sum_{k=1}^{N-1} \frac{(2\sigma\omega\lambda_k)}{(\omega)^2 + (2\sigma\lambda_k)^2} \tag{7}$$

where N is the number of monomers and ν represents the number of monomers per unit volume in the solution and $\sigma = 3k_B T/\zeta l^2$. λ_k are the nonzero eigenvalues of matrix $[\boldsymbol{H}.\boldsymbol{A}]$, which are directly proportional to the relaxation rates as $(1/\tau_k = 2\sigma\lambda_k)$ and inversely proportional to the relaxation times (τ_k). It is important to note that the factor of 2 in the relaxation rates originates from the second moment of the displacements involved in computing the stress required in the evaluation of $G^*(\omega)$.[15] The storage modulus comprises the elastic contribution that measures the ability of a polymer to store energy due to deformation. Meanwhile, the loss modulus is the viscous part that accounts for energy dissipation as heat. It is widely accepted, based on linear-response theory and thermodynamic principles, that eqs 6 and 7 for the storage and loss moduli are universally applicable.[33,34] Consequently, these equations are valid regardless of the variations in the topology of the polymer chain and its composition. Therefore,

https://doi.org/10.1021/acs.jpcb.4c05788
J. Phys. Chem. B 2025, 129, 496−505

eqs 6 and 7 are also applicable for the ring copolymers, where the heterogeneity affects only the relaxation times.

3. RESULTS AND DISCUSSION

The properties of the alternating ring copolymer depend on the eigenvalues of matrix $[\boldsymbol{H.A}]$. Figure 2 represents the double logarithmic plot of the eigenvalues of matrix $[\boldsymbol{H.A}]$ versus N/k for various sizes of the ring copolymer. The mode number, k, denotes the segments comprising N/k monomers. Small mode numbers represent large segments that correspond to collective relaxation modes. Large mode numbers represent small segments that correspond to local relaxation modes. Due to the periodic symmetry of ring copolymers, the odd modes vanish, while the eigenvalues corresponding to the even modes are double degenerate. Therefore, Figure 2 displays the eigenvalues with even modes only. The viscoelastic relaxation rates, $1/\tau_k$, of the normal relaxation modes are directly proportional to their respective eigenvalues, λ_k. The ring copolymer consisting of different sized monomers possesses different relaxation rates, leading to two distinct eigenvalue zones corresponding to the local and collective relaxation rates. For small mode numbers, the eigenvalues are similar to those of the homopolymeric rings,[11] while at large mode numbers, the eigenvalues of the ring copolymer cluster in a specific region of the log−log plot, which is absent in the ring homopolymer. The local relaxation rates corresponding to large mode numbers are considerably higher than the collective relaxation rates at small mode numbers. The difference in the eigenvalues at large mode numbers for various ring sizes is highlighted in the inset of Figure 2.

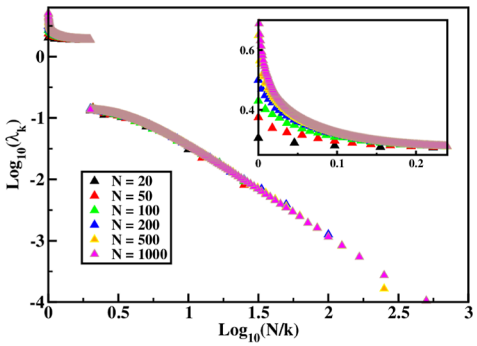

Figure 2. Eigenvalues of the ring copolymer with HI for various ring sizes as a function of length scale, N/k, with $\zeta_B = 5\zeta_A$. The inset shows the variation in eigenvalues at large mode numbers.

Figure 3 displays a double logarithmic plot of the storage and loss moduli for the ring copolymer as a function of the normalized frequency, $\omega\tau_1$, both with and without HI. It may be observed that $[G'(\omega)]$ and $[G''(\omega)]$ display three different regimes represented by the low, high, and intermediate frequencies. Both storage and loss moduli exhibit universal scaling behavior in the low and high frequency regimes. The behavior of these moduli in low and high frequency regimes may be understood from the limiting results of eqs 6 and 7. At the low frequency regime

$$[G'(\omega)] = \lim_{\omega\to 0}\left(\sum_{k=1}^{N-1}\frac{(\omega)^2}{(\omega)^2 + (2\sigma\lambda_k)^2}\right) \simeq \sum_{k=1}^{N-1}\frac{(\omega)^2}{(2\sigma\lambda_k)^2} \sim (\omega)^2 \tag{8}$$

and

$$[G''(\omega)] = \lim_{\omega\to 0}\left(\sum_{k=1}^{N-1}\frac{(2\sigma\omega\lambda_k)}{(\omega)^2 + (2\sigma\lambda_k)^2}\right) \simeq \sum_{k=1}^{N-1}\frac{(\omega)}{(2\sigma\lambda_k)} \sim (\omega) \tag{9}$$

At the high frequency regime

$$[G'(\omega)] = \lim_{\omega\to \infty}\left(\sum_{k=1}^{N-1}\frac{(\omega)^2}{(\omega)^2 + (2\sigma\lambda_k)^2}\right) \simeq \sum_{k=1}^{N-1}\frac{(\omega)^2}{(\omega)^2} \sim (\omega)^0 \tag{10}$$

and

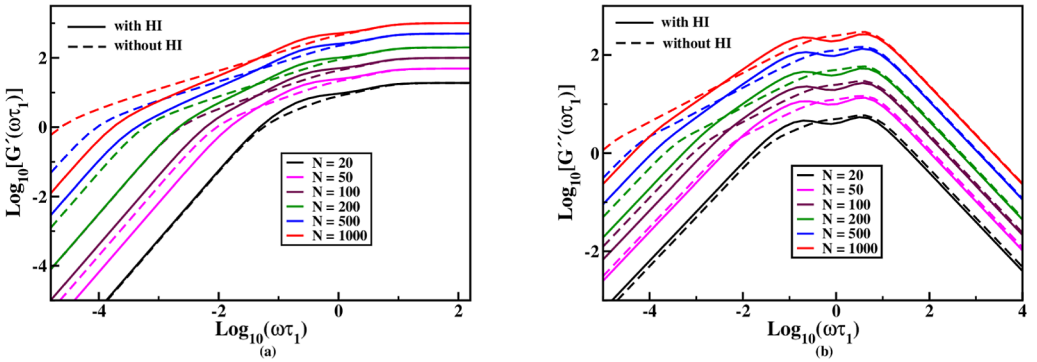

Figure 3. Double logarithmic plots of storage and loss moduli of ring copolymers as a function of normalized frequency, $\omega\tau_1$, for various ring sizes with $\zeta_B = 5\zeta_A$.

https://doi.org/10.1021/acs.jpcb.4c05788
J. Phys. Chem. B 2025, 129, 496−505

$$[G''(\omega)] = \lim_{\omega\to\infty}\left(\sum_{k=1}^{N-1}\frac{(2\sigma\omega\lambda_k)}{(\omega)^2 + (2\sigma\lambda_k)^2}\right)$$
$$\simeq \sum_{k=1}^{N-1}\frac{(2\sigma\lambda_k)}{(\omega)}$$
$$\sim (\omega)^{-1} \quad (11)$$

The storage modulus varies as $[G'(\omega)] \sim (\omega)^2$ in the low frequency regime and is independent of frequency in the high frequency regime. The loss modulus linearly increases and decreases with frequency in the low and high frequency regimes, respectively, with a maximum in the intermediate frequency regime. Typically, the structure-dependent behavior is reflected in the intermediate frequency regime. The variation of these frequency-dependent mechanical relaxation moduli may be expressed in terms of the eigenvalues (λ_k), which are directly proportional to the corresponding relaxation rates ($1/\tau_k$) of the normal relaxation modes. In the low frequency regime, $[G'(\omega)]$ and $[G''(\omega)]$ scale with eigenvalues as $[G'(\omega)] \sim (\lambda_k)^{-2}$ and $[G''(\omega)] \sim (\lambda_k)^{-1}$, respectively. Thus, the mechanical relaxation moduli are dominated by the lower nonzero eigenvalues in the low frequency regime, which denote the smaller relaxation rates corresponding to the collective relaxation modes. In the high frequency regime, $[G'(\omega)]$ is independent of the eigenvalues, whereas $[G''(\omega)]$ varies with eigenvalues as $[G''(\omega)] \sim (\lambda_k)$. Thus, $[G''(\omega)]$ is dominated by higher eigenvalues with high relaxation rates that correspond to the local relaxation modes.

The magnitudes of $[G'(\omega)]$ and $[G''(\omega)]$ increase with an increase in the size of the ring copolymer due to a corresponding increase in the number of normal relaxation modes. In the low frequency regime, the magnitude of $[G'(\omega)]$ and $[G''(\omega)]$ for the ring copolymers is lower in the presence of HI than that in its absence. This is due to an increase in the lower relaxation rates in the presence of HI. This difference increases with an increase in the size due to an increase in the number of lower relaxation rates, while in the high frequency regime, $[G''(\omega)]$ is dominated by the higher relaxation rates and the magnitude of $[G''(\omega)]$ decreases in the presence of HI, suggesting that HI decreases the higher relaxation rates corresponding to the local relaxation modes.

For a particular size of the ring copolymer, the plots of the storage modulus both with and without HI merge in the high frequency regime, depicting a constant value of $[G'(\omega)]$. One crossover is observed for $[G'(\omega)]$ in the intermediate frequency regime, while $[G''(\omega)]$ of a large ring copolymer displays two crossovers in the intermediate frequency regime, and $[G''(\omega)]$ of a small ring (N = 20) shows only one crossover. The structure-dependent behavior of the ring copolymers lies in the intermediate frequency regime, where $[G'(\omega)] \sim (\omega)^{\alpha_1}$ and $[G''(\omega)] \sim (\omega)^{\alpha_2}$. The values of these scaling exponents for the linear polymers are 0.66 and 0.5 with and without HI, respectively.[15] Table 1 lists the values of the exponents α_1 and α_2 for the ring copolymer in the presence and absence of HI. For the ring copolymers, α_1 and α_2 decrease and increase, respectively, with an increase in ring size, which is similar to that of the ring homopolymers.[29] In the absence of HI, α_1 and α_2 are similar to the exponents of the linear polymer chains. In the presence of HI, α_2 for the large sized rings is similar to the exponent of the linear polymer, while α_1 shows a notable deviation. The ring copolymers exhibit the same power law behavior as that of the ring homopolymers in both low and high frequency regimes.[29]

Table 1. Scaling Exponents of the Storage and Loss Moduli, $[G'(\omega)] \sim (\omega)^{\alpha_1}$ and $[G''(\omega)] \sim (\omega)^{\alpha_2}$, of the Ring Copolymers in the Presence and Absence of HI in the Intermediate Frequency Regime With $\zeta_B = 5\zeta_A$

N_{total}	$\alpha_1^{[A]}$	$\alpha_1^{[H,A]}$	$\alpha_2^{[A]}$	$\alpha_2^{[H,A]}$
200	0.558	0.846	0.490	0.642
500	0.536	0.772	0.494	0.644
1000	0.522	0.746	0.495	0.650

The intermediate frequency regime is dominated by the intermediate eigenvalues, representing the multimode relaxation. In the presence of HI, $[G'(\omega)]$ shows quasi-plateau behavior for the ring copolymers, which is reminiscent of a more solid-like behavior, and $[G''(\omega)]$ exhibits a bimodal behavior with two maxima due to the difference in the mobilities of the A- and B-type monomers. At the low frequency region, the dynamics of the ring copolymer is accelerated in the presence of HI, which may be explained from the smallest nonzero eigenvalue representing the smallest relaxation rate. The smallest nonzero eigenvalue (λ_{N-1}) of the ring copolymer for N = 1000 is 1.3159×10^{-5}, which on inclusion of HI increases by an order of magnitude to 1.0526×10^{-4}.

It is interesting to compare the frequency-dependent viscoelastic responses of the ring copolymers of various sizes both with and without HI. This is done by comparing $[G'(\omega)]$ and $[G''(\omega)]$ as a function of the normalized frequency, $\omega\tau_1$. Figure 4 depicts a double logarithmic plot comparing $[G'(\omega)]$ and $[G''(\omega)]$ for the ring copolymers. For a particular sized ring, $[G'(\omega)]$ and $[G''(\omega)]$ exhibit crossovers in the intermediate frequency regime. The frequency corresponding to this crossover is called the crossover frequency, ω_c, at which $[G'(\omega)] = [G''(\omega)]$, representing a crossover between the liquid-like viscosity and solid-like elasticity. At low frequencies, the ring exhibits a liquid-like viscous behavior at frequencies below the ω_c i.e., $\omega < \omega_c$ and $[G'(\omega)] < [G''(\omega)]$. A solid-like elastic behavior is observed at higher frequencies above the ω_c i.e., $\omega > \omega_c$ and $[G'(\omega)] > [G''(\omega)]$. It indicates that the viscoelastic behavior of ring copolymers is predominantly viscous and elastic in the low and high frequency regimes, respectively. This characteristic crossover frequency is different with and without HI and does not occur at $\omega\tau_1 = 1$, which is predicted for the single relaxation time of a Maxwell fluid, suggesting that these ring copolymers exhibit multimode relaxation. It occurs at $\omega\tau_1 \approx 1$ for lower generation dendrimers, as found in theoretical[35] and experimental studies.[36] For star polymers, it occurs at $\omega\tau_1 \approx 4$[37] and at $\omega\tau_1 < 1$ and $1 < \omega\tau_1 < 4$ for large and small sized Rouse rings,[29] respectively. This characteristic crossover occurs at $\omega\tau_1 < 1$ for all sizes of the ring copolymers both with and without HI, as seen from Figure 4. Thus, it may be concluded that the ring copolymers are less compact than the corresponding linear and ring homopolymers. This crossover frequency shifts to lower frequencies with increasing ring sizes. A marginal shift to lower frequencies is noted in the presence of HI.

The effects of the size and HI on the viscoelastic spectrum of the ring copolymers are measured via the loss tangent ($\tan\delta$), which quantifies the energy dissipated during an oscillatory deformation relative to the stored elastic energy. Figure 5 depicts the double logarithmic plot of $\tan\delta$ as a function of the

https://doi.org/10.1021/acs.jpcb.4c05788
J. Phys. Chem. B 2025, 129, 496−505

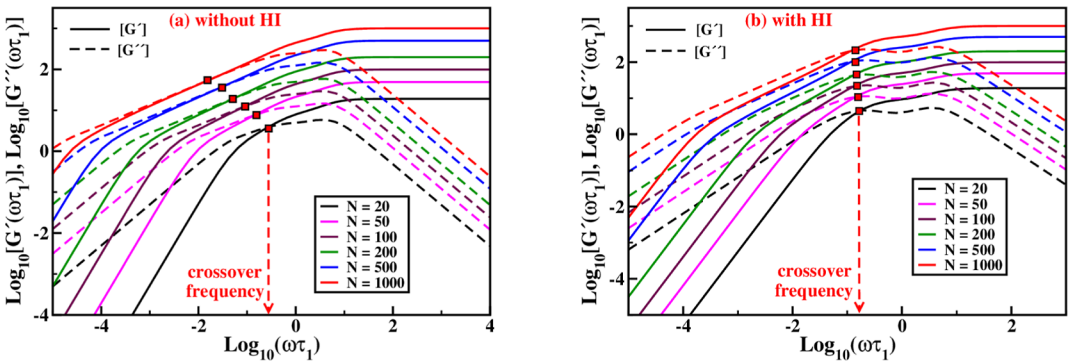

Figure 4. Comparison of the storage and loss moduli of the ring copolymer (a) without HI and (b) with HI for various ring sizes with $\zeta_B = 5\zeta_A$.

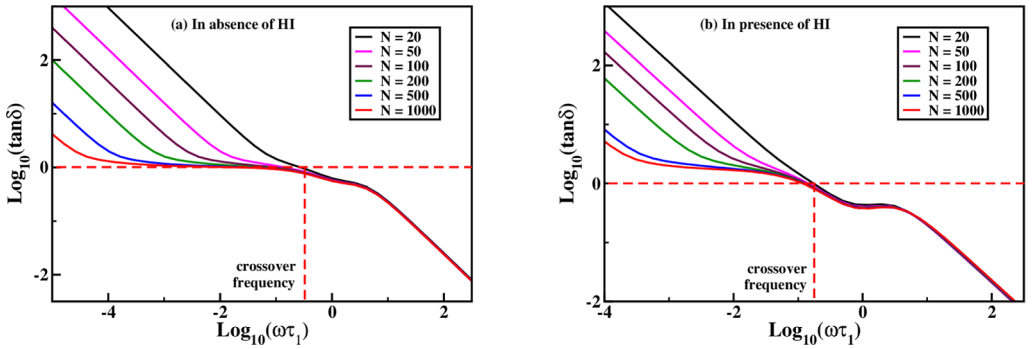

Figure 5. Double logarithmic plot of loss tangent (tan δ) versus normalized frequency, $\omega\tau_1$, for ring copolymers with and without HI with $\zeta_B = 5\zeta_A$.

normalized frequency, $\omega\tau_1$, for the ring copolymers with and without HI. A small change in the ring size has a more pronounced effect on the loss tangent in the low frequency regime, while in the high frequency regime, all curves merge, showing that the loss tangent is independent of the ring size. The loss tangent decreases sharply and plateaus off before merging. This frequency-independent plateau occurs at a higher frequency for small sized rings. This denotes the transition from a viscoelastic liquid to a viscoelastic solid. Similar behavior was observed in the crystallizing polymers, where the loss tangent drops precipitously with the crystallizing parameter as the polymer approaches a purely elastic response.[38] A precise understanding of the magnitude of the crossover frequencies can be obtained by examining the loss tangent, tan δ. The frequency at which $[G'(\omega)] = [G''(\omega)]$ represents the crossover frequency, (ω_c). However, on a logarithmic scale, $\log_{10}\tan(\delta) = 0$ corresponds to crossover frequency, (ω_c), marked by the red line in the figure. From Figure 5, it may be seen that the crossover frequency decreases with an increase in the ring size both with and without HI. This is because large polymers exhibit more solid-like behavior at lower frequencies. However, this decrease in the crossover frequency is very small in the presence of HI.

The crossover frequency is closely related to the characteristic relaxation time of the polymer, which measures the time scale at which the transition from predominantly viscous to predominantly elastic behavior occurs in a polymer. This characteristic relaxation time may be approximated as the inverse of the crossover frequency $\tau^* = 1/(\omega_c)$. The reduced characteristic relaxation times for ring copolymers with and without HI are presented in Table 2 for different ring sizes. It may be noted that the characteristic relaxation times increase with an increase in the ring size, corresponding to a slower relaxation. The characteristic relaxation time of small sized ring copolymers is higher in the presence of HI, while it is lower for the larger ones. This may be due to the weaker strength of HI in smaller rings. An increase in the strength of HI increases the smaller relaxation rates corresponding to the collective relaxation modes and decreases the relaxation time. However, an increase in the ring size tends to increase the characteristic relaxation time. Due to the two counteracting trends, the increase in the characteristic relaxation times is much smaller for the large sized rings with HI than that for the rings without HI. The ring copolymers have a higher relaxation time because of larger B-type monomers relative to that of a ring homopolymer with only A-type (smaller) monomers.[29]

Table 2. Characteristic Overall Relaxation Times of Ring Copolymers of Various Sizes with $\zeta_B = 5\zeta_A$

N_{total}	τ^*_A	$\tau^*_{H.A}$
20	3.162	6.026
50	4.786	6.607
100	11.220	7.499
200	16.218	7.727
500	24.547	8.254
1000	60.256	8.484

The effect of increasing the number of B-type monomers in a ring copolymer of a particular size, $N_{total} = 1000$, is studied by varying the number of B-type monomers from 250 to 600 to generate three block ring copolymers with different values of ρ, i.e., $\rho = 0.25$, 0.4, and 0.6. For block ring copolymers, the mean square bond lengths are chosen to be different for the bonds between B−B, A−B, and A−A type monomers as $l_{B-B} > l_{A-B} > l_{A-A}$, which makes the corresponding spring constants different. Figure 6 represents the double logarithmic plot of the storage and loss moduli for the ring copolymers ($N_{total} = 1000$) as a function of the normalized frequency for different values of ρ.

https://doi.org/10.1021/acs.jpcb.4c05788
J. Phys. Chem. B 2025, 129, 496−505

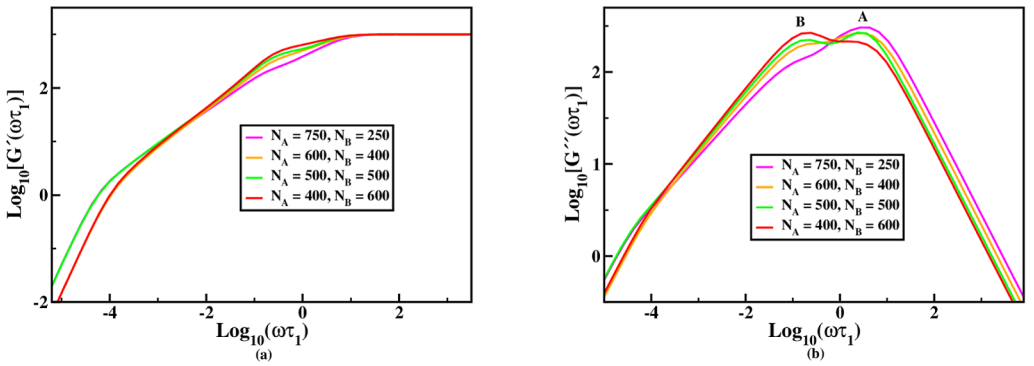

Figure 6. Double logarithmic plot of storage and loss moduli of ring copolymers as a function of normalized frequency with different number fractions of B-type monomers in an N_{total} = 1000 sized ring copolymer with $\zeta_B = 5\zeta_A$.

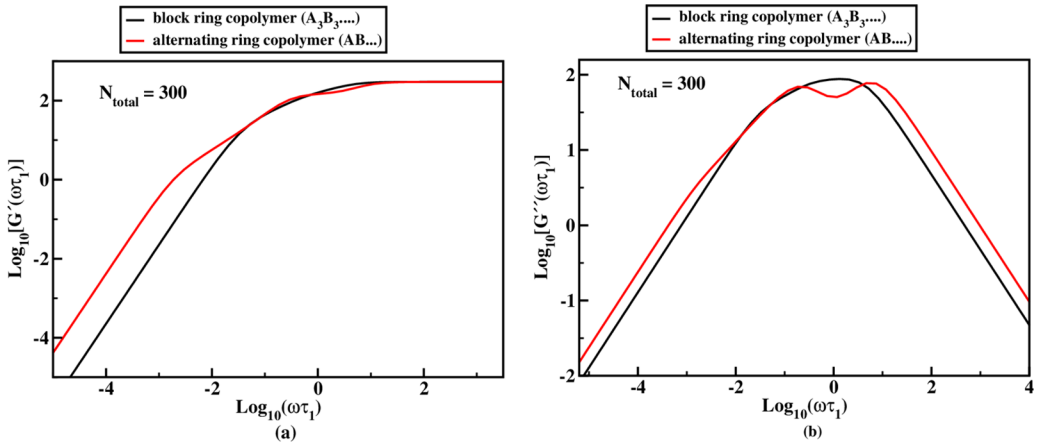

Figure 7. Comparison of storage and loss moduli of the alternating ring copolymer ($ABAB$...) and block ring copolymer ($A_3B_3A_3B_3$...) with HI for N_{total} = 300 with $\zeta_B = 5\zeta_A$.

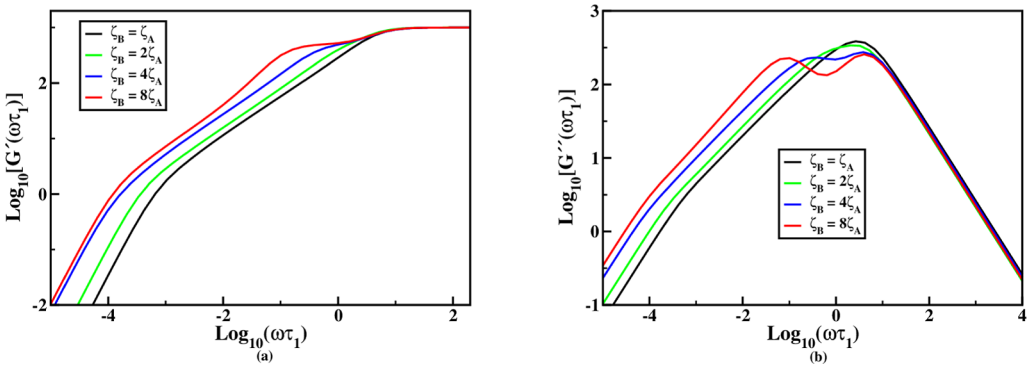

Figure 8. Double logarithmic plot of storage and loss moduli of ring copolymers as a function of normalized frequency by varying the friction coefficient of the B-type monomer ($\zeta_B = \zeta_A$, $2\zeta_A$, $4\zeta_A$, $8\zeta_A$).

It is evident from Figure 6 that B-type monomers have a significant effect on the viscoelastic properties, even at lower number fractions. With an increase in ρ, the storage modulus $[G'(\omega)]$ increases at intermediate frequencies, while the loss modulus $[G''(\omega)]$ shows an appreciable increase in the intermediate frequency regime, followed by a decrease at higher frequencies. Both $[G'(\omega)]$ and $[G''(\omega)]$ follow a power law behavior in the intermediate frequency regime as $[G'(\omega)] \sim (\omega)^{\alpha_1}$ and $[G''(\omega)] \sim (\omega)^{\alpha_2}$. An increase in the number of B-type monomers increases scaling exponents α_1 and α_2. However, the ring copolymer with $\rho = 0.4$ shows a higher value of α_1. In the intermediate frequency regime, $[G'(\omega)]$ shows a quasi-plateau that is enhanced with an increase in the number of B-type monomers. This indicates a transition from liquid-like to solid-like behavior. Therefore, with an increase in ρ, the ring copolymers show more solid-like behavior. At higher frequencies, the effect of the number of B-type monomers is relatively weak on $[G'(\omega)]$. These results suggest that the B-type (larger) monomers influence the stress relaxation dynamics more than the plateau modulus. Remarkably, the effect of larger monomers is more pronounced on the loss modulus than on the storage modulus. For the loss modulus, an increase in the number fraction of B-type (larger) monomers results in the appearance of a second maximum

https://doi.org/10.1021/acs.jpcb.4c05788
J. Phys. Chem. B 2025, 129, 496−505

at a lower frequency. These maxima are due to the larger monomers, which have a lower mobility. The two maxima have similar amplitudes for an equal number of A- and B-type monomers in the ring copolymer. The splitting between the maxima remains unaltered by changing the number fraction of the B-type monomers.

A comparison between the storage and loss moduli of the alternating ring copolymer ($ABAB...$) and block ring copolymer ($A_3B_3A_3B_3...$) with HI is depicted in Figure 7. In the low frequency regime, the magnitude of both the storage and loss moduli decrease for the block ring copolymer compared to those of the alternating ring copolymer. This decrease is higher for the storage modulus relative to that of the loss modulus as the storage and loss moduli vary as $[G'(\omega)] \sim (\lambda_k)^{-2}$ and $[G''(\omega)] \sim (\lambda_k)^{-1}$, respectively, in the low frequency regime. Therefore, the smaller relaxation rates increase in the block ring copolymer ($A_3B_3A_3B_3...$). In the high frequency regime, the magnitude of the storage modulus remains unaltered as $[G'(\omega)] \sim (\lambda_k)^0$, while the magnitude of the loss modulus is lower for the block ring copolymer, which corresponds to a decrease in the higher relaxation rates. The topological features of any polymer are reflected in the intermediate frequency regime. In this regime, the block ring copolymers lack the quasi-plateau and bimodal trend in the storage and loss moduli, respectively, unlike those of alternating ring copolymers. Therefore, the block ring copolymers are structurally different from the alternating ring copolymers.

Figure 8 displays the storage and loss moduli, $[G'(\omega)]$ and $[G''(\omega)]$, of the ring copolymer with $N_{total} = 1000$ and $\rho = 0.5$ in the presence of HI for various sizes of the B-type monomers. The size of the B-type monomers is varied up to 8 times that of the A-type monomers. The ring where the size of B-type monomers is equal to the size of A-type monomers, $\zeta_B = \zeta_A$, corresponds to a ring homopolymer (black line) and reproduces the corresponding eigenvalues. For such rings, $[G'(\omega)]$ exhibits power law behavior $[G'(\omega)] \sim \omega^{0.697}$ in the intermediate frequency regime (10^{-3} to 10^{0}), while $[G'(\omega)] \sim \omega^2$ in the low frequency region and displays a constant value at the high frequency domain. These bounding regimes represent the universal scaling behavior of $[G'(\omega)]$ in the low and high frequency regions. Similarly, $[G''(\omega)]$ also obeys power law behavior $[G''(\omega)] \sim \omega^{0.618}$ in the intermediate frequency regime and exhibits universal scaling behavior in the low and high frequency regimes. The scaling exponents for various sizes of B-type monomers in the ring copolymers in the intermediate frequency regime are given in Table 3. Both scaling exponents α_1 and α_2 increase with an increase in the size of B-type monomers. In the low frequency regime, the size of the B-type monomer drastically affects both moduli, $[G'(\omega)]$ and $[G''(\omega)]$, while in the high frequency regime, all curves coincide with each other. An increase in the size of B-type monomers enhances the viscoelastic behavior of polymers by enhancing both $[G'(\omega)]$ and $[G''(\omega)]$ in the low frequency regime. For $\zeta_B > \zeta_A$, the A-type monomers are more mobile than the B-type monomers, and the dynamics is slower than that of ring homopolymers with only A-type (smaller) monomers. $[G'(\omega)]$ displays a quasi-plateau regime with different sizes of B-type monomers ($\zeta_B = 2\zeta_A, 4\zeta_A, 8\zeta_A$), and this quasi-plateau region is pronounced for the larger B-type monomers, indicating a liquid to solid-like transition. The loss modulus for $\zeta_B > \zeta_A$, i.e., for the ring copolymer with $\zeta_B = 4\zeta_A, 8\zeta_A$ shows a second maximum at lower frequencies due to a difference in the mobilities of the A- and B-type monomers. The split between the maxima increases with an increase in the size of the B-type monomers. Similar behavior is observed in the case of ring copolymers without HI and dendrimers.[39,40]

The effect of different sizes of B-type monomers on the crossover frequency of the ring copolymers in the presence of HI is depicted in Figure 9. It may be observed that the crossover frequency decreases with an increase in the size of the B-type monomers, suggesting that at lower frequencies, the ring copolymers with larger B-type monomers exhibit more solid-like behavior. An increase in the relaxation time with size is compensated by an increase in the strength of the HI, similar to the behavior of the loss tangent. Here, the size of the ring is fixed so that the effect of the size of the B-type monomer and the effect of HI can be observed. Table 3 presents the reduced characteristic relaxation time for the corresponding crossover frequency using equation $\tau^*_{H.A} = 1/(\omega_c)$. The relaxation times here vary appreciably. Copolymers with larger B-type monomers have higher relaxation times. Such ring copolymers have a lower mobility and slower dynamics. This lower mobility further contributes to a decrease in the crossover frequency. It may be concluded that the crossover frequency and the characteristic relaxation times of the ring copolymers with different B-type monomers are primarily governed by the size of the B-type monomers rather than HI.

The effect of incorporating the fluctuations in HI in linear polymers was reported earlier using Gaussian approximation,[19] which agreed well with the results of the Brownian dynamics simulations.[41,42] When fluctuations are included, both the storage and loss moduli decrease at low frequencies. However, at high frequencies, the storage modulus is the same as that

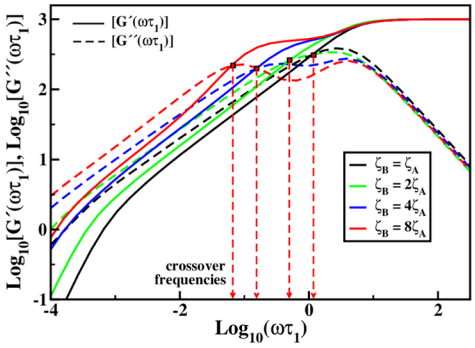

Figure 9. Comparison of storage and loss moduli of ring copolymers as a function of normalized frequency by varying the friction coefficient of the B-type monomer ($\zeta_B = \zeta_A, 2\zeta_A, 4\zeta_A, 8\zeta_A$).

Table 3. Scaling Exponent (α_1 and α_2) of $[G'(\omega)]$ and $[G''(\omega)]$, Respectively, and the Characteristic Overall Relaxation Times of Ring Copolymers with HI for Various Sizes of the B-Type Monomer ($\zeta_B = n\zeta_A$ With n = 1, 2, 4, 8)[a]

$\zeta_B = n\zeta_A$	α_1	α_2	$\tau^*_{H.A}$
$\zeta_B = \zeta_A$	0.697	0.618	1.122
$\zeta_B = 2\zeta_A$	0.711	0.634	1.897
$\zeta_B = 4\zeta_A$	0.714	0.636	6.310
$\zeta_B = 8\zeta_A$	0.783	0.691	15.400

[a]These scaling exponents are extracted from the slopes of the straight lines by fitting the intermediate frequency regime for different values of N.

https://doi.org/10.1021/acs.jpcb.4c05788
J. Phys. Chem. B 2025, 129, 496−505

predicted by the Rouse−Zimm model, while the loss modulus is enhanced.[19]

4. CONCLUSIONS

In this work, we present a multiresolution model of ring copolymers within the framework of the optimized Rouse−Zimm theory. The multiresolution feature arises from differently sized beads with different friction coefficients that are connected through different harmonic springs. The model represents larger beads as B-type monomers and smaller beads as A-type monomers. The HI between the pair of monomers are approximated by using the preaveraged HI tensors. For ring polymers, inclusion of fluctuations in HI may decrease the magnitude of both storage and loss moduli at low frequencies, as in linear polymers. The mechanical relaxation moduli are evaluated from this multiresolution model, which provides an insight into the rheology of the ring copolymers. The frequency-dependent loss and storage moduli are evaluated as a function of the ring size, HI, number fraction, and size of the B-type monomers. The mechanical relaxation moduli depend only on the eigenvalues, which are determined from the numerical diagonalization of the $[\boldsymbol{H.A}]$ matrix. In the low frequency regime, both storage and loss moduli are dominated by the lower relaxation rates corresponding to the collective relaxation modes, while in the high frequency regime, the loss modulus is dominated by higher relaxation rates corresponding to local relaxation modes. The HI increase the smaller relaxation rates corresponding to collective relaxation modes, which accelerates the overall relaxation dynamics. The higher relaxation rates corresponding to local relaxation modes decrease with HI and the characteristic maxima shift to a lower frequency. In the presence of HI, $[G'(\omega)]$ shows a quasi-plateau, which is reminiscent of a more solid-like behavior, while $[G''(\omega)]$ exhibits two maxima due to the difference in the mobilities of two types of monomers. The dynamical ranges of both storage and loss moduli are reduced in the low frequency regime, which indicates accelerated dynamics in the presence of HI.

The viscoelastic response of the ring copolymers is predominantly viscous in the low frequency regime and elastic in the high frequency regime. The characteristic crossover for the ring copolymers occurs at $\omega\tau_1 < 1$, suggesting that the ring copolymers are less compact as compared to the linear and ring homopolymers and represent the multimode Maxwell model. The inverse of the crossover frequency represents the characteristic overall relaxation time. The characteristic relaxation time for large sized rings is lower for the rings with HI, suggesting enhanced dynamics in the presence of HI. The ring copolymers in the absence of HI exhibit a slower relaxation due to the larger size of one of the monomers as compared to the bare Rouse rings. The storage and the loss moduli are also evaluated as a function of the number fraction and size of two different types of monomers for a particular ring size.

The quasi-plateau in $[G'(\omega)]$ increases with an increase in the size and number fraction of B-type monomers, leading to a transition from the liquid to a solid-like behavior in the intermediate frequency regime. The loss modulus shows a second maximum due to a difference in the mobilities of the two types of monomers, which is enhanced with the number fraction and size of the larger monomer. The splitting between the maxima remains unchanged on changing the number fraction, while it increases with the size of the larger monomers. Both storage and loss moduli increase with an increase in the size of the larger monomers in the low frequency regime, indicating a slow relaxation dynamics of ring copolymers as compared to the ring homopolymers with only A-type (smaller) monomers. This slow relaxation may be characterized in terms of the relaxation times, which vary appreciably with the size of the larger monomers.

■ ASSOCIATED CONTENT

Data Availability Statement

The data that support the findings of this study are available in the article.

■ AUTHOR INFORMATION

Corresponding Author

Parbati Biswas − *Department of Chemistry, University of Delhi, Delhi, Delhi 110007, India;* orcid.org/0000-0001-7709-2263; Email: pbiswas@chemistry.du.ac.in

Author

Sumit Kumar − *Department of Chemistry, University of Delhi, Delhi, Delhi 110007, India*

Complete contact information is available at: https://pubs.acs.org/10.1021/acs.jpcb.4c05788

Notes

The authors declare no competing financial interest.

■ ACKNOWLEDGMENTS

The authors gratefully acknowledge the DST-SERB, India (Project no. CRG/2022/000889) for providing the financial support. S.K. acknowledges CSIR, India, for providing financial assistance in the form of Senior Research Fellowship [File No: 09/045(1785)/2020-EMR-I].

■ REFERENCES

(1) Tubiana, L.; Alexander, G. P.; Barbensi, A.; Buck, D.; Cartwright, J. H.; Chwastyk, M.; Cieplak, M.; Coluzza, I.; Čopar, S.; Craik, D. J.; et al. Topology in soft and biological matter. *Phys. Rep.* **2024**, *1075*, 1−137.

(2) Jeong, Y.; Jin, Y.; Chang, T.; Uhlik, F.; Roovers, J. Intrinsic viscosity of cyclic polystyrene. *Macromolecules* **2017**, *50*, 7770−7776.

(3) Lloyd, E. M.; Lopez Hernandez, H.; Feinberg, E. C.; Yourdkhani, M.; Zen, E. K.; Mejia, E. B.; Sottos, N. R.; Moore, J. S.; White, S. R. Fully recyclable metastable polymers and composites. *Chem. Mater.* **2019**, *31*, 398−406.

(4) Miao, Z.; Kubo, T.; Pal, D.; Sumerlin, B. S.; Veige, A. S. pH-responsive water-soluble cyclic polymer. *Macromolecules* **2019**, *52*, 6260−6265.

(5) Martínez-Tong, D. E.; Ochs, J.; Barroso-Bujans, F.; Alegria, A. Broadband dielectric spectroscopy to validate architectural features in Type-A polymers: Revisiting the poly (glycidyl phenyl ether) case. *Eur. Phys. J. E* **2019**, *42*, 93.

(6) Kapnistos, M.; Lang, M.; Vlassopoulos, D.; Pyckhout-Hintzen, W.; Richter, D.; Cho, D.; Chang, T.; Rubinstein, M. Unexpected power-law stress relaxation of entangled ring polymers. *Nat. Mater.* **2008**, *7*, 997−1002.

(7) Watanabe, H.; Inoue, T.; Matsumiya, Y. Transient Conformational Change of Bead- Spring Ring Chain during Creep Process. *Macromolecules* **2006**, *39*, 5419−5426.

(8) Richter, D.; Gooßen, S.; Wischnewski, A. Celebrating Soft Matter's 10th Anniversary: Topology matters: structure and dynamics of ring polymers. *Soft Matter* **2015**, *11*, 8535−8549.

(9) Rosa, A.; Orlandini, E.; Tubiana, L.; Micheletti, C. Structure and dynamics of ring polymers: Entanglement effects because of solution density and ring topology. *Macromolecules* **2011**, *44*, 8668−8680.
(10) Kwon, Y.; Matsumiya, Y.; Watanabe, H. Viscoelastic and orientational relaxation of linear and ring rouse chains undergoing reversible end-association and dissociation. *Macromolecules* **2016**, *49*, 3593−3607.
(11) Handa, M.; Biswas, P. Conformations of ring polymers with excluded volume interactions. *J. Rheol.* **2021**, *65*, 595−604.
(12) Rolls, E.; Togashi, Y.; Erban, R. Varying the resolution of the Rouse model on temporal and spatial scales: Application to multiscale modeling of DNA dynamics. *Multiscale Model. Simul.* **2017**, *15*, 1672−1693.
(13) Neha; Biswas, P.; Kant, R. Theory for the Dynamics of Polymer Grafted Nanoparticle in Solution. *J. Phys. Chem. C* **2019**, *123*, 30657−30665.
(14) Neha; Kant, R. Static Structure Factor and Viscoelastic Properties of Dendrimer Grafted Nanoparticles in Solution. *J. Phys. Chem. B* **2021**, *125*, 1951−1959.
(15) Doi, M.; Edwards, S. F. *The Theory of Polymer Dynamics*; Clarendon Press Oxford, 1986.
(16) Yamakawa, H. *Modern Theory of Polymer Solutions*; Harper & Row, 1971.
(17) Rotne, J.; Prager, S. Variational treatment of hydrodynamic interaction in polymers. *J. Chem. Phys.* **1969**, *50*, 4831−4837.
(18) Yamakawa, H. Transport properties of polymer chains in dilute solution: hydrodynamic interaction. *J. Chem. Phys.* **1970**, *53*, 436−443.
(19) Öttinger, H. C. Gaussian approximation for Rouse chains with hydrodynamic interaction. *J. Chem. Phys.* **1989**, *90*, 463−473.
(20) Zimm, B. H. Dynamics of polymer molecules in dilute solution: viscoelasticity, flow birefringence and dielectric loss. *J. Chem. Phys.* **1956**, *24*, 269−278.
(21) Chen, Z. Y.; Cai, C. Dynamics of starburst dendrimers. *Macromolecules* **1999**, *32*, 5423−5434.
(22) Rolls, E.; Erban, R. Multi-resolution polymer Brownian dynamics with hydrodynamic interactions. *J. Chem. Phys.* **2018**, *148*, 194111.
(23) Osaki, K.; Schrag, J. L.; Ferry, J. D. Infinite-dilution viscoelastic properties of poly (α-methylstyrene). applications of Zimm theory with exact eigenvalues. *Macromolecules* **1972**, *5*, 144−147.
(24) Perico, A. Segmental relaxation in macromolecules. *Acc. Chem. Res.* **1989**, *22*, 336−342.
(25) Press, W. H.; Vetterling, W. T.; Teukolsky, S. A.; Flannery, B. P. *Numerical Recipes in Fortran*; Cambridge University Press: Cambridge, U.K., 1992.
(26) Liu, T. W.; Öttinger, H. C. Bead-spring rings with hydrodynamic interaction. *J. Chem. Phys.* **1987**, *87*, 3131−3136.
(27) Handa, M.; Biswas, P. Segmental mobility of ring polymers in good and poor solvents. *Macromolecules* **2022**, *55*, 2182−2192.
(28) Kumar, S.; Biswas, P. Intrinsic viscosity and dielectric relaxation of ring polymers in dilute solutions. *J. Chem. Phys.* **2023**, *159*, 164902.
(29) Handa, M.; Biswas, P. Intramolecular relaxation of ring polymers in dilute solutions. *J. Rheol.* **2021**, *65*, 381−390.
(30) Ferry, J. D. *Viscoelastic Properties of Polymers*; John Wiley & Sons, 1980.
(31) Kumar, A.; Biswas, P. Intramolecular relaxation dynamics in semiflexible dendrimers. *J. Chem. Phys.* **2011**, *134*, 214901.
(32) Kumar, A.; Rai, G. J.; Biswas, P. Conformation and intramolecular relaxation dynamics of semiflexible randomly hyperbranched polymers. *J. Chem. Phys.* **2013**, *138*, 104902.
(33) Stockmayer, W.; Kennedy, J. Viscoelastic spectrum of free-draining block copolymers. *Macromolecules* **1975**, *8*, 351−355.
(34) Man, V. F.; Schrag, J. L.; Lodge, T. P. Bead-spring model calculations of the viscoelastic and oscillatory flow birefringence properties of block copolymer solutions. *Macromolecules* **1991**, *24*, 3666−3680.
(35) Rai, G. J.; Kumar, A.; Biswas, P. Intramolecular relaxation of flexible dendrimers with excluded volume. *J. Chem. Phys.* **2014**, *141*, 034902.
(36) Uppuluri, S.; Morrison, F. A.; Dvornic, P. R. Rheology of dendrimers. 2. Bulk polyamidoamine dendrimers under steady shear, creep, and dynamic oscillatory shear. *Macromolecules* **2000**, *33*, 2551−2560.
(37) Pearson, D. S.; Helfand, E. Viscoelastic properties of star-shaped polymers. *Macromolecules* **1984**, *17*, 888−895.
(38) Kotula, A. A frequency-dependent effective medium model for the rheology of crystallizing polymers. *J. Rheol.* **2020**, *64*, 505−515.
(39) Satmarel, C.; Gurtovenko, A. A.; Blumen, A. Viscoelastic relaxation of cross-linked, alternating copolymers in the free-draining limit. *Macromolecules* **2003**, *36*, 486−494.
(40) Satmarel, C.; Gurtovenko, A. A.; Blumen, A. Relaxation of copolymeric dendrimers built from alternating monomers. *Macromol. Theory Simul.* **2004**, *13*, 487−496.
(41) Zylka, W.; Öttinger, H. C. A comparison between simulations and various approximations for Hookean dumbbells with hydrodynamic interaction. *J. Chem. Phys.* **1989**, *90*, 474−480.
(42) Schroeder, C. M. Single polymer dynamics for molecular rheology. *J. Rheol.* **2018**, *62*, 371−403.

https://doi.org/10.1021/acs.jpcb.4c05788
J. Phys. Chem. B 2025, 129, 496−505